Proceedings of the 25th International Conference on
Port and Ocean Engineering under Arctic Conditions
June 9-13, 2019, Delft, The Netherlands

High pressure crushing of ice against a concrete surface under confined conditions

Jeremy Costello[1], Yiran Liu[2], Stephen Bruneau[2], Bruce Colbourne[2]
[1] Memorial University of Newfoundland and Labrador, St. John's, Canada
[2] Memorial University of Newfoundland and Labrador, St. John's, Canada

ABSTRACT

The goal of the ICEWEAR* research program is to enhance understanding of ice-induced wear on concrete surfaces in polar marine environments, and, to develop design strategies for wear resistance. Laboratory experiments simulating high pressure ice crushing and extrusion are the subject of this paper. These experiments were conducted to observe the behavior of confined ice advancing towards a concrete surface, to observe the effects of the interaction on the concrete surface, and to validate aspects of the experimental apparatus for use in the design of advanced wear testing equipment.

A specialized extrusion frame was designed, built and then mounted on an MTS machine in a cold room at Memorial's thermodynamics laboratory. The extrusion frame facilitated the loading of ice cylinders into a steel tube positioned vertically over a concrete surface. The ice was driven through the tube into the concrete surface by means of a piston threaded onto the MTS machine's hydraulic actuator. Ice was thereby crushed, spalled or otherwise extruded through the gap between the confining tube and the concrete surface. The independent variables for the experimental program were gap distance and rate of advance. The dependent variables were thrust force, ice behavior and concrete surface wear. Thrust force was measured via a load cell on the piston, whereas video and still photography, including photo microscopy techniques were the primary tools for observing ice crushing and concrete wear.

**ICEWEAR "Ice Wear and Abrasion Effects on Concrete Surfaces" MUN, Kvaerner, NLIC, NSERC(CRD) 2017-2022.*

KEY WORDS: Ice; Concrete; Wear; Extrusion; Confinement

INTRODUCTION

This research is part of a larger project (ICEWEAR* 2017-2022) that is exploring the nature of ice-induced wear of concrete surfaces in polar marine environments. Prior work in this area through laboratory experimentation is found in the literature under Itoh et al., 1988, Huovinen, 1993, Hanada et al., 1996 and Fioro et al., 2005, and more recently under Moen et al., 2015 and Tijsen et al., 2015. Bekker et al., 2011 have looked at wear rates for sliding abrasion on concrete samples. The work of Jacobsen et al., 2015 has advanced the understanding of processes through modelling and prediction of long-term wear. Much of the recent work is on the sliding abrasion of ice on concrete, while not much has been done on the compressive crushing of ice against concrete or the combination of crushing and sliding. No work has been reported for wear in wet environments. Ryan (2017) proposed an alternative testing strategy using a rotary motion device which may facilitate long duration wear processes at high pressures under dry or submerged conditions. One element of that concept was the ice delivery mechanism or ice extruder as it has been called. This paper highlights experiments that were designed to test the ice extrusion mechanism concept for the future ice wear machine, while giving insight into the behavior of ice and concrete under extreme loading conditions.

EXPERIMENT

The experiments were conducted inside a cold room at Memorial University between -11ºC and -13ºC. The equipment consisted of an MTS machine with high a capacity load cell, extrusion apparatus and various optical recording devices (microscope, camera, and GoPro). Figure 1 shows the extrusion apparatus installed on the cold room MTS machine prior to a test.

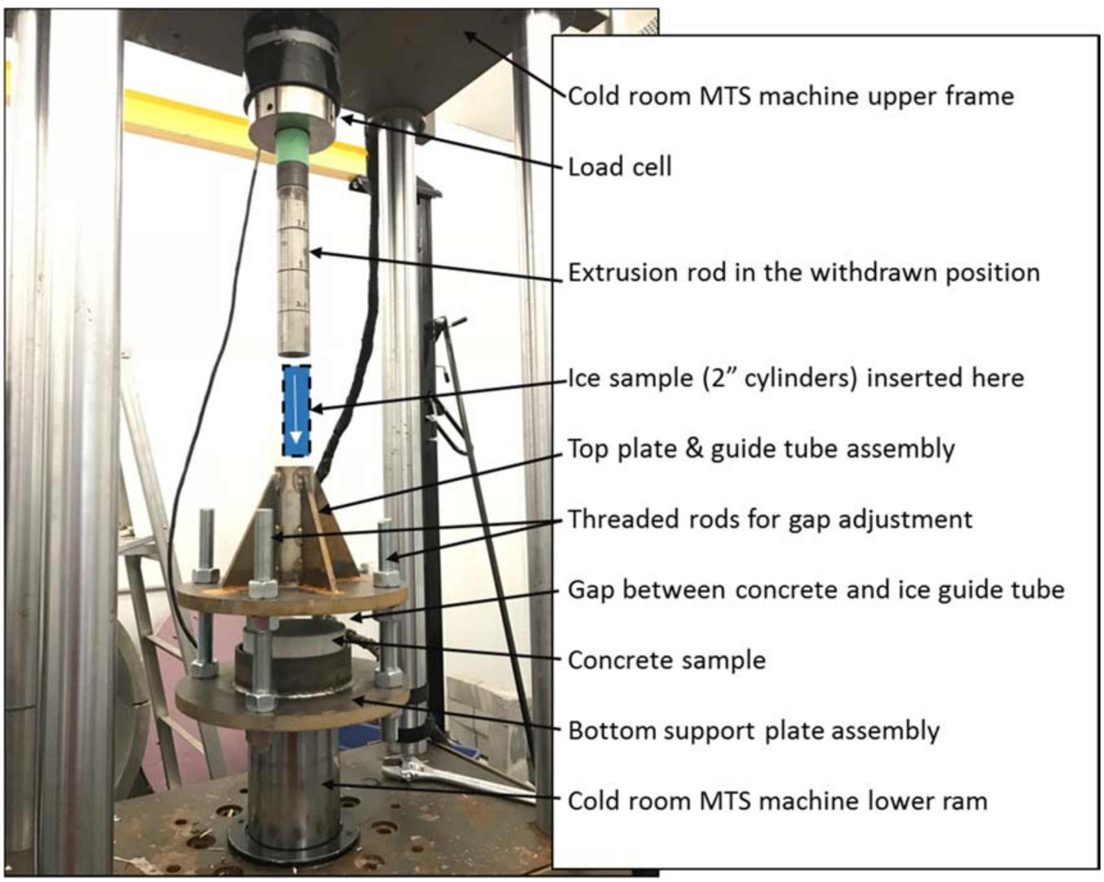

Figure 1. Cold room MTS machine with extrusion apparatus installed

The salient features of the extrusion apparatus are: robustness for safety and integrity of the work; ease of assembly and integration with existing MTS machine, simplicity of ice and concrete sample replacement, and, an adjustable gap between the concrete surface and the bottom of the ice guide tube (the unconfined span). The extrusion apparatus was made of welded 1020 steel plate and pipe, and 1” diameter Grade A threaded rod and nuts. The apparatus advances the ice at a pre-determined controlled rate by moving the entire lower assembly, ice and all, upwards into the extrusion rod, causing the ice to be pushed through the cylinder and crushed against the concrete sample. The average inner diameter of the ice guide tube was 53.1mm. Other features and documentation can be found in Liu, (2018).

Recording Devices

Load and displacement were recorded using the in-house DAQ system and a high sampling rate of 2000Hz was used to capture event frequencies up to 1 Mhz. Three optical devices were used to document processes visually. A GoPro HERO3 provided video recording of each test, backlit by LED lights. The GoPro was attached to the top plate of the test apparatus using a c-clamp, so that it travelled with the frame capturing the relative motion of the ice. A Dino-Lite Edge AM7915MZT USB microscope was used to take close-up pictures of the concrete before and after each set of experiments in order to observe and qualify any damage caused to the concrete by the high-pressure extrusion. The microscope is equipped with extended depth of field capabilities, but the changes in the concrete were too small to take advantage of this. General pictures of the experimental setup and aftermath were taken using a 5-megapixel cell phone camera.

Ice Preparation

Ice samples were freshwater and were prepared using the methodology reported in Bruneau et al (2013) and Ryan (2017). The objective was to obtain uniform, competent (uncracked) and reproducible samples of ice representative of natural polycrystalline formation. The method involves the use of machine-produced (filtered water) ice pellets which are then passed through a chipping machine. The chips are poured into molds (two-inch diameter by four-inch long plastic cylinders) which are themselves positioned in a customized Styrofoam insulation block so that the bases of the plastic molds remain uninsulated.

De-aerated, deionized and distilled fresh water is then mixed in with the ice chip seeds, stirring as they are mixed in order to remove air bubbles. An insulating lid is placed over the open-ended tops of the plastic molds and the assembly is set in a freezer. This arrangement facilitates bottom-up, unconfined ice growth which eliminates stress cracks and reduces air entrapment. Once frozen, the plastic cylinders are removed from the Styrofoam insulation block. A hole is drilled in the bottom of the plastic cylinder and compressed air is used to blow the plastic cylinder off the ice. The ice samples are then stored individually in airtight bags until test time. Rough ice samples ranged in diameter from 49.46 to 52.35mm and in length from 84.82 to 98.18mm (Figure 2). A cold-room band saw was typically used to square the sample ends.

Figure 2. Two inch by four inch cylindrical ice samples

Concrete Preparation

Normal strength concrete was prepared using W/C of 0.5, a C/F of 1.2, and a V% of between 4 and 6%. The aggregate size was 10mm. A standard 4x8 inch cylinder form was used after which the cylinder was cured for three weeks and then cut into three-inch long specimens. For these pilot tests the flat-cut surface of the concrete was to be the contact surface. The cut concrete surface (Figure 3) rather than the formed surface (mostly mortar) is more representative of a naturally worn surface and may better reveal differential abrasion patterns between aggregate and mortar.

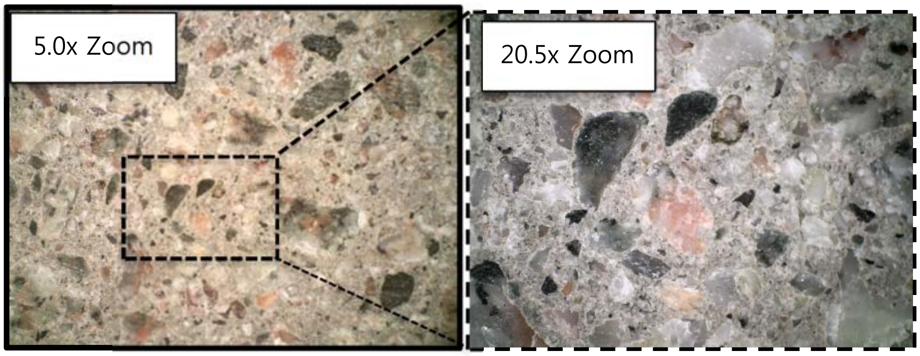

Figure 3. Cut surface of a concrete sample

Experimental Procedure

Equipment, ice and concrete samples were kept in the cold room to acclimatize at -11 to -13C for one day. The test plan was to vary advance rate by selecting between 0.5 and 2.5 mm/s and to vary the gap spacing between 6 and 25 mm. A test proceeded by inserting the concrete sample, setting the gap via positioning of the nuts on the threaded rods and then sliding two ice specimens down the guide tube so that the exposed end of the leading ice sample came to rest against the concrete surface. The extrusion rod was then manually advanced down into the tube and halted prior to making contact with the ice. All recording equipment was then readied and the cold room vacated. The triggering of a test almost immediately resulted in the growth of load as the extrusion rod made contact with the ice and compressive forces grew. Of primary concern during these tests was excessive load accumulation due to over-confined ice and excessive friction inside the tube. Thus the first extrusion tests were conducted at a comfortable 25mm gap between tube and concrete, and the slow advance rate of 0.5mm/s enabled the interruption of the ongoing test if loads approached the working load cell limit of 500KN. The first test indicated loads well within machine limits so it was allowed to proceed to the target advance distance of 100mm – well short of the 150-200mm of ice in the tube.

RESULTS

The maximum force and equivalent pressure for each test is shown in Table 1. The highest loads (over 200 kN) were achieved at the slowest speeds with the least gap opening. Likewise the lowest loads (less than 10 kN) resulted from higher speed extrusions with a wide gap.

The tests with gap spacing of 6 and 12mm and extrusion speed of 2.5mm/s behaved similarly, with high amounts of “sawtoothing” gradually increasing in force over the course of the test. Sawtoothing is when the force builds up until a small part of the ice fails, causing a sharp drop in the force. The force then builds up until another small part of the ice fails and this keeps repeating. The graph of this phenomenon looks like a sawtooth. The force data from the test with a gap spacing of 6mm and extrusion speed of 2.5mm/s, shown in Figure 4, illustrates this. The test with 25mm gap spacing and 2.5mm/s extrusion speed had similar amounts of sawtoothing but had no force buildup (Figure 5). This is due to the large space for the ice to escape removing any possible resistance to the ice coming out through the gap.

Table 1. Maximum Force and Pressure

Test Run	Spacing (mm)	Speed (mm/s)	Max Force (kN)	Max Pressure (MPa)
1	25	0.5	15	7.0
2	25	2.5	6	2.6
3	12	0.5	184	82.9
4	12	2.5	24	11.0
5	6	0.5	182	82.3
6	6	2.5	58	26.4
7	6	0.5	211	95.2
8	6	2.5	54	24.6
9	12	0.5	204	92.3
10	12	0.5	193	87.0
11	12	2.5	12	5.6
12	25	0.5	23	10.2
13	25	2.5	4	2.0

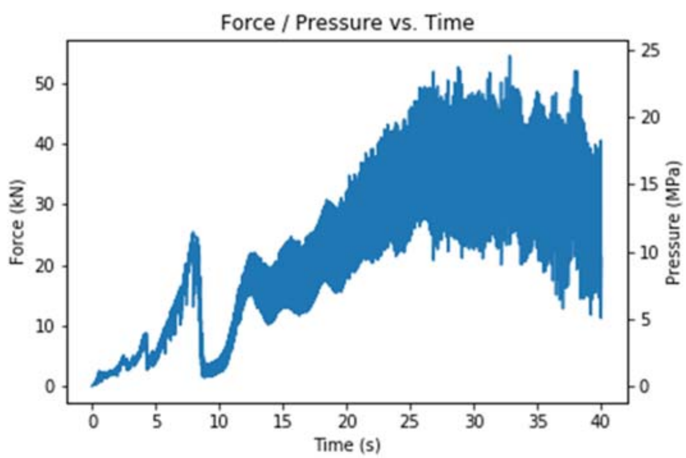

Figure 4. 6mm Gap spacing, 2.5mm/s extrusion speed

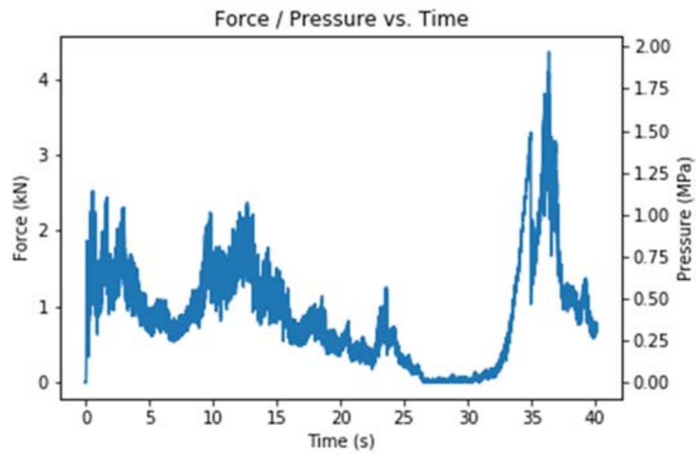

Figure 5. 25mm Gap spacing, 2.5mm/s extrusion speed

The test with 25mm gap spacing and 0.5mm/s extrusion speed had very little sawtoothing aside from the first few seconds and had relatively smooth force buildup throughout the test (Figure 6). This is due to the ice acting as a ductile material and being slowly deformed through compression as the force increases until the ice bulges and collapses out the gap. Thus it appears that the transition from brittle to ductile failure has been captured in the test program.

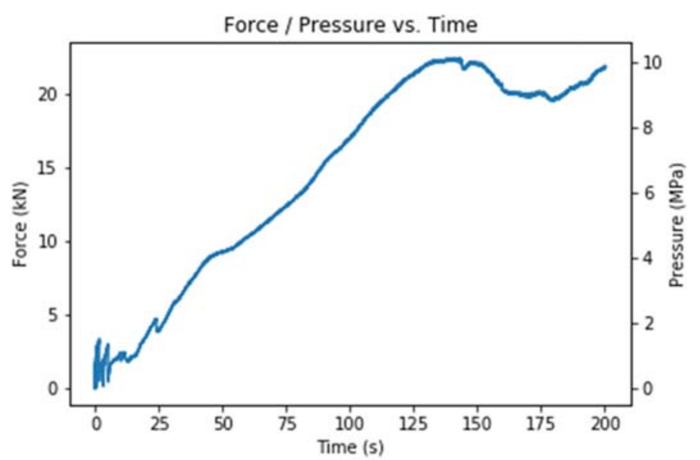

Figure *6*. 25mm Gap spacing, 0.5mm/s extrusion speed

The tests with gap spacing of 6 and 12mm and extrusion speed of 0.5mm/s were somewhat like the 25mm & 0.5mm/s test (Figure 6) in appearance except that the peak force was an order of magnitude higher. The peak was very similar for the 6 and 12mm gap spacing at slow speeds: 210.86kN for the 6 mm and 198.62kN for the 12 mm. It was also observed the high peak force for these tests was invariably followed by a smooth force decline as extrusion continued. It was hypothesized that this decline was a result of the reduced length of the sample remaining in tube subject to wall friction. This is discussed later in this paper.

The relationship between maximum pressure, advance rate and gap spacing is illustrated in Figure 7.

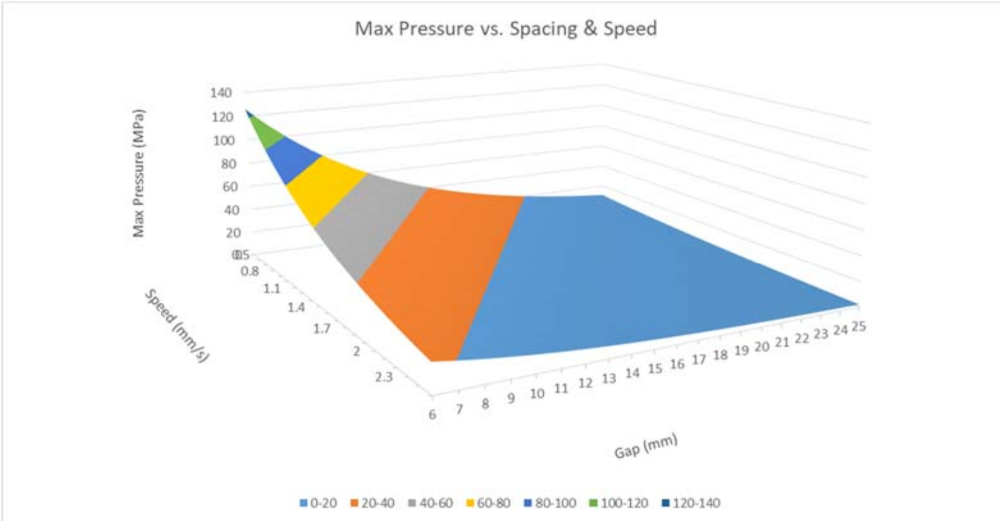

Figure 7. Max Pressure vs. Spacing & Speed

The data illustrated in Figure 7 was fit with a two-variable logarithmic regression:

$$y = b{m_1}^{x_1}{m_2}^{x_2} \tag{1}$$

Where x1 is the gap spacing in mm, and x2 is the extrusion speed in mm/s. The regression variable values rounded to five significant figures are shown in the following table.

Table 2. Regression Variable Values

Regression Variable	Value
b	419.68
m_1	0.87908
m_2	0.42247

This regression model has an R^2 value of 0.93915, and an F-statistic value of 77.165. The chi-square p-value of the model was calculated to be 1.0859e-10. The degrees of freedom for the numerator (df1) and denominator (df2) were calculated as follows, where k is the number of independent variables and n is the population size. The independent variables are gap spacing and extrusion speed, so k is 2, and the population size (n) is 13,

$$df_1 = k - 1 = 2 - 1 = 1 \tag{2}$$

$$df_2 = n - k - 1 = 13 - 2 - 1 = 10 \tag{3}$$

With an alpha value of 0.001, the F-critical value is 21.040. Since the p-value is less than the alpha value and the F-statistic is greater than the F-critical value, the p-value is less than the alpha value of 0.001. This means that the result is significant.

More tests could be performed in the future to validate or improve upon these results as the population size of 13 is small, and there were only two extrusion speeds varied during testing. Tests can also be performed over a wider range, as this model may not extrapolate well.

Test Phase Analysis

For the 6mm and 12mm gap spacing at a speed of 0.5mm/s the ice is compressed and then forced out through the gap following a load pattern exemplified in Figure 8. The pattern appears to go through four phases: sawtoothing (1), build-up (2), peak (3), and load decay (4).

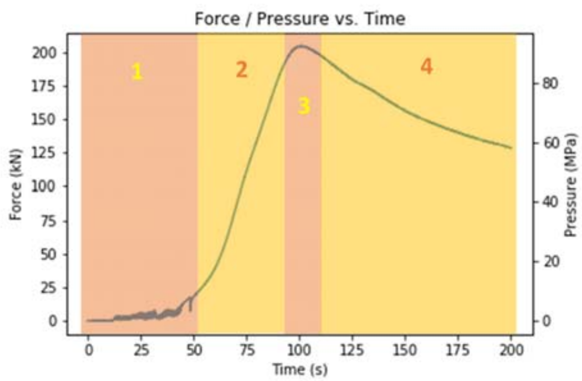

Figure 8. 12mm Gap spacing, 0.5mm/s extrusion speed

An illustration of what is thought to be happening within the guide tube during each stage of this test is shown below. These inferences were made based on observing simultaneous and synchronized video and load trace information.

1 – Sawtoothing

Ice begins cracking and shows cycles of small breaks followed by sharp drops in force, then a slower build-up to another small break.

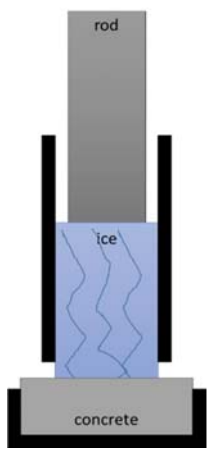

2 – Linear Load Build-up

Ice is crushed, causing a change in the structure of the ice, represented by the colour change.

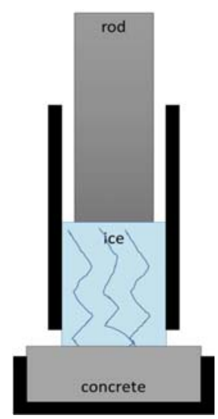

3 – Load Plateaus

Ice begins to leak out the side as the force peaks.

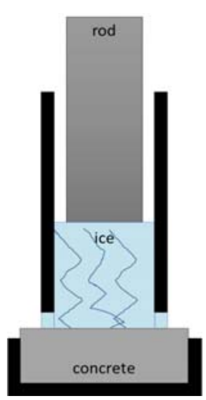

4 – Load Drops due to Drop in Friction

Force declines due to the decrease friction in the tube as more ice is pushed out through the gap.

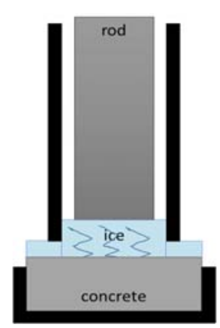

Failure Mechanism Analysis

One would assume that the ice is compressed uniformly during the test, but this was not the case in these tests. A small amount of ice was remaining at the end of each test, one of which is pictured below. These pictures are from a test with gap spacing of 12mm and extrusion speed of 0.5mm/s.

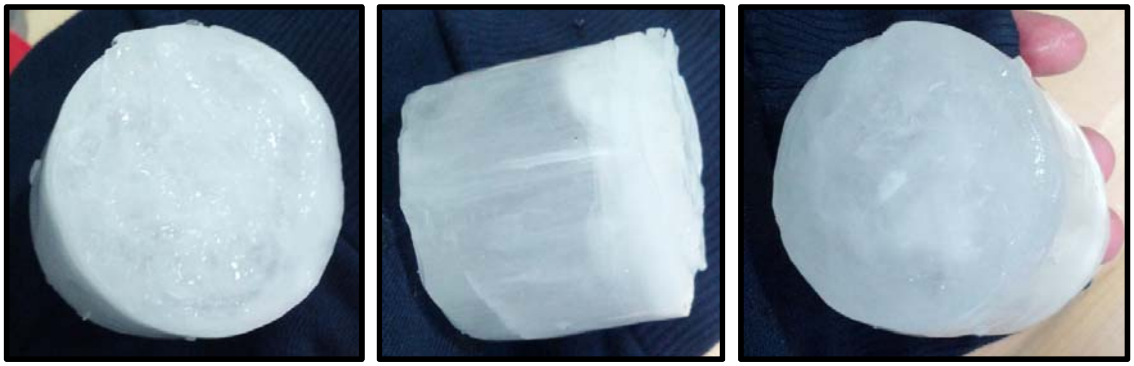

Figure 10. Low speed test remainder portion of ice specimen.

The whiter end was the end exposed to the concrete, while the clearer end was the end touching the extrusion rod inside the tube. The part of the ice still contained within the upper plate cylinder appears to have changed, but not to the extent of the part of the ice that was close to or within the gap.

The ice came out through the gap during the tests with extrusion speed of 0.5mm/s in a radial finger pattern, as can be seen in Figure 11. The thickness of the splayed ice decreased as the gap spacing decreased. The 6mm gap height resulted in many thin radial fingers, the 12mm gap height resulted in some medium-sized radial fingers, while the 25mm gap height resulted in a small number of large radial fingers. During these slower tests, the ice acted like a ductile material and experienced deformation similar to plastic deformation.

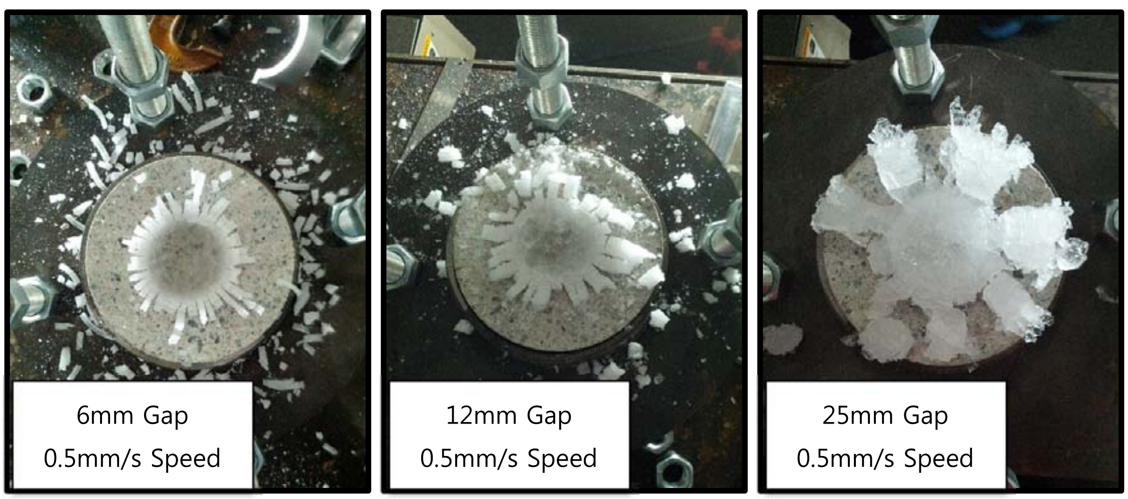

Figure 11. Ice extrusion patterns remaining after tests.

In contrast to the 0.5mm/s rate results the tests at an extrusion rate of 2.5mm/s resulted in the ice being ejected as crushed rubble in a brittle-like fashion. For these faster tests, the rubble grain size decreased as gap spacing decreased as observed in Figure 12.

Figure 12. Post-test Rubble

The ice stump remaining in the tube after the 2.5mm/s extrusion speed tests were more jagged than the flat ice stumps left from 0.5mm/s extrusion tests. This shows that the ice is shattered and spalled away by being pushed into the concrete during the faster tests, whereas it is compressed into the concrete until failure during the slower tests. This may be due to the higher amounts of vibration during the higher extrusion speed tests caused by the higher magnitude of sawtoothing force fluctuation and the faster crushing speed. Pictures of the ice stump after a 25mm gap spacing and 2.5mm/s extrusion rate test is shown in Figure 13.

Figure 13. High-speed Test Ice Stump

Friction Extraction Analysis

In an effort to isolate the ice crushing/concrete reaction forces from the total measured force an effort was made to extract the contribution of ice/wall friction. It was observed that the slow speed tests with gap spacing of 6 and 12mm reached a peak force and then declined in a pattern resembling exponential decay. Assuming that the interaction between the ice and concrete had reached a steady state condition, the assumption was made that the declining load was a result of the shortening of the ice specimen sliding against the wall of the tube. Thus it was proposed to find the theoretical asymptote of this decline – the point at which the remaining ice specimen no longer touched the tube (a condition we did not risk executing in the lab). This decline was fitted using an exponential equation, and the extrapolated asymptotic force and equivalent pressure were calculated at distant time (10000 seconds). These values are shown in Table 3.

Table 3. Extrapolated Friction Force and Pressure

Run	Spacing (mm)	Speed (mm/s)	Extrapolated Force (kN)	Extrapolated Pressure (MPa)
5	6	0.5	96.26	43.44
7	6	0.5	88.39	39.89
9	12	0.5	99.93	45.1
10	12	0.5	91.83	41.44

The curve fit for the first 12mm gap height and 0.5mm/s extrusion speed is shown in Figure 14. The blue line is the measured force data while the orange line is a theoretical 500 second extrapolation.

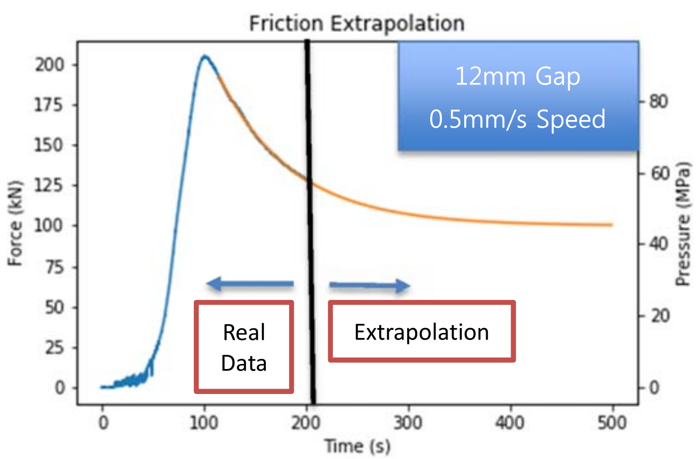

Figure 14. Friction Extrapolation

Remarkably, the asymptotic limit force appears to be fixed around 90 to 100 kN resulting in a nominal pressure between 40 and 45 MPa. Under the circumstances and conditions of these tests this pressure may be interpreted as the steady state interaction between fully crushed and transformed ice and the concrete surface – irrespective of gap spacing within the small gap range. The non-linear form of the load drop might be a result of the decline of resistive wall-friction forces within the tube due to simultaneous decline of confinement pressure and contact area. Open-end effects also interfere with a growing portion of the ice specimen remaining in the tube further contributing to non-linearities in resistive force. It is also possible that temperature effects resulting from the high pressures and friction had some influence on the pattern of load reduction as extrusion progressed. If more tests are to be undertaken the apparatus will be fitted out with another load cell beneath the concrete specimen so that the ice-concrete interaction forces may be unambiguously measured.

CONCLUSIONS

A simple apparatus for extruding ice at high pressures onto a concrete surface has been tested. The execution of the tests was not difficult, however, the approach was shown to have its limits insofar as being a practical delivery mechanism for ice at crushing pressures is concerned. Ice extruded unto an unyielding surface resulted in the crushing of the ice sample throughout its entire volume inducing pressures inside the walls of the guide tube leading to undesirable friction forces. None-the-less as a means of thrusting ice towards a concrete surface, moving or not, at pressures less than that which causes the ice to crush and spall, the mechanism may prove useful.

The attempt to survey the concrete sample after each test proved to be inconclusive. A more rigorous and convenient optical measurement procedure is required as the removal of the sample was awkward and the cold room availability was time-limited. After every extrusion test there was some ice debris left plastered to the concrete, which raised the question of how to remove it without affecting abrasion, or whether removing it is in fact one of the natural abrasion mechanisms. It also became apparent that multiple tests would be required to induce wear that could be appreciably measured or even detected using the optical means at our disposal. The attempt to use microscopy was thus abandoned for these pilot tests.

The tests provided some insight into the nature of confined ice behavior. It is not unrealistic to consider the setup as one that simulates aspects of high pressure zones known to occur within a wider crushing interface. In these tests the rate of extrusion and the degree of confinement were varied systematically. For the faster tests with an extrusion speed of 2.5mm/s, the force variations were very large and sawtoothing occurred throughout the entire test. The ice shattered and spalled against the concrete in a brittle fashion. The ejected ice was rubble-like when not highly confined, and powder-like when confined. The slower tests with an extrusion speed of 0.5mm/s were much smoother and the ice failed in a ductile manner. The extruded ice exiting the gap was in the shape of coherent radial fingers, with the size of the fingers increasing with the gap spacing.

Across the board, the maximum force and pressure for the tests increased as both the extrusion speed and gap spacing decreased. The tests with gap spacing of 6mm and 12mm exhibited similar load growth and decline patterns. Through a theoretical extrapolation it was suggested that the extrusion pressure due to impingement on the concrete alone reaches a steady state constant value near 40-45 MPa for gap spacing between 6 and 12mm. Discriminating concrete/ice forces from ice/steel friction forces was a complication that may in the future be avoided if a separate load cell were placed beneath the concrete specimen. It might also be of interest to attempt these tests with a pressure film at the concrete interface to illuminate the nature of the pressure distribution within the highly confined contact zone.

REFERENCES

Abdelnour R., Comfort G., Malik L., & Sumner K., 2006. Ice Abrasion Tests of Metal Based Coatings. *Proc. of the 18th IAHR Int. Symp. on Ice,* pp.277-285.

Bekker, A., Uvarova, T., Pomnikov, E., Farafonov, A., Prytkov, I., & Tyutrin, R., 2011. Experimental Study of Concrete Resistance to Ice Abrasion. *International Offshore and Polar Engineering Conference*, Maui, pp.1044-1047.

Fiorio, B., Meyssonnier, J., & Boulon, M., 2002. Experimental Study of the Friction of Ice Over Concrete Under Simplified Ice-structure Interaction Conditions. *Canadian Journal of Civil Engineering*, 29, pp.347-359.

Fiorio, B., 2005. Wear Characterization and Degradation Mechanisms of a Concrete Surface Under Ice Friction. *Construction and Building Materials*, 19, pp.366-375.

Hanada, M., Ujihira, M., Hara, F., & Saeki, H., 1996. Abrasion rate of various materials due to the movement of ice sheets. *Proceedings of The Sixth International Offshore and Polar Engineering Conference*, pp. 433-437.

Hoff, G., 1989. Evaluation of Ice Abrasion of High-Strength Lightweight Concrete for Arctic Applications. *Offshore Mechanics and Arctic Engineering Conference*, Hague, pp.583-590.

Huovinen, S., 1990. Abrasion of Concrete by Ice in Arctic Sea Structures. *Journal of Structural Mechanics*, 23, pp.23-35.

Huovinen, S., 1993. Abrasion of Concrete Structures by Ice. *Cement and Concrete Research*, 23, pp.69-82.

Itoh, Y., Yoshida, A., Tsuchiya, M., Katoh, K., Sasaki, K., & Saeki, H., 1988. An Experimental Study on Abrasion of Concrete Due to Sea Ice. *Offshore Technology Conference*, Houston, pp.61-68.

Jacobsen, S., Scherer, G., & Schulson, E., 2015. Concrete-ice Abrasion Mechanics. *Cement and Concrete Research*, 73, pp.79-95.

Jia, Q. et al., 2011. Experimental Study on Adhesion Strength of Freshwater Ice Frozen to Concrete Slab. *Advanced Materials Research*, 243-249, pp.4587-4591.

Liu, Y., 2018. *Ice Extrusion Machine Design and Lab Test.* Undergraduate. St. John’s: Memorial University of Newfoundland and Labrador.

Møen, E., Høiseth, K., Leira, B., & Høyland, K., 2015. Experimental Study of Concrete Abrasion due to Ice Friction - Part I: Set-up, Ice Abrasion vs. Material Properties and Exposure Conditions. *Cold Regions Science and Technology*, 110, pp.183-201.

Nawwar, A., & Malhotra, V., 1988. Development of a Test Method to Determine the Resistance of Concrete to Ice Abrasion and/or Impact. *American Concrete Institute*, 109, pp.401-426.

Ryan, A., 2017. ICE WEAR AND ABRASION OF MARINE CONCRETE: Design of Experimental Apparatus and Procedures. M.Eng Thesis. St. John’s, NL. Memorial University.

Shamsutdinova, Guzel & Hendriks, Max & Jacobsen, Stefan., 2017. Concrete-Ice Abrasion Laboratory Experiments. *Proceedings - International Conference on Port and Ocean Engineering under Arctic Conditions*, Busan, pp.42-48.

Tijsen, J., Bruneau, S., & Colbourne, B., 2015. Laboratory Examination of Ice Loads and Effects on Concrete Surfaces from Bi-axial Collision and Adhesion Events. *Proceedings - International Conference on Port and Ocean Engineering under Arctic Conditions*, Trondheim, pp.183-195.

Tijsen, J., 2015. Experimental Study on the Development of Abrasion at Offshore Concrete Structures in Ice Conditions. Master's Thesis. Delft: Delft University of Technology.